

NASA-CR-196436

19745

Neotectonics of Asia: Thin-shell finite-element models with faults

by Xianghong Kong and Peter Bird
Department of Earth and Space Sciences
University of California
Los Angeles, CA 90024

NAGW-2042

1-46

(NASA-CR-196436) NEOTECTONICS OF
ASIA: THIN-SHELL FINITE-ELEMENT
MODELS WITH FAULTS (California
Univ.) 46 p

N95-12949

Unclass

G3/46 0019745

Submitted to Tectonic Evolution of Asia, a Rubey volume edited by An Yin and
T. Mark Harrison, to be published by Cambridge University Press.

July 1994

PRECEDING PAGE BLANK NOT FILMED

ABSTRACT

As India has pushed into and beneath the south margin of Asia in Cenozoic time, it has added a great volume of crust, which may have been either (i) emplaced locally beneath Tibet, (ii) distributed as regional crustal thickening of Asia, (iii) converted to mantle eclogite by high-pressure metamorphism, or (iv) extruded eastward to increase the area of Asia. The amount of eastward extrusion or "escape" is especially controversial: plane-stress computer models of finite strain in a continuum lithosphere have shown minimal escape, while laboratory and theoretical plane-strain models of finite strain in a faulted lithosphere have shown escape as the dominant mode. We suggest that the best way to work toward a resolution is to study the present (or *neo*)tectonics by a set of computational experiments, making use of the known fault network and using available data on fault activity, geodesy, and stress to select the best model.

We apply a new thin-shell method which can represent faulted lithosphere of realistic rheology on a sphere, and provide predictions of present velocities, fault slip-rates, and stresses for various trial rheologies and boundary conditions. To minimize artificial boundaries, the models include all of Asia east of 40°E and span 100° on the globe. The primary unknowns are the friction coefficient of faults within Asia and the amounts of shear traction applied to Asia in the Himalayan and oceanic subduction zones around its margins. Data on Quaternary fault activity prove to be most useful in rating the models.

The best results are obtained with very low fault friction of 0.085 (only 10% of the friction assumed within unfaulted blocks): this major heterogeneity shows that unfaulted continuum models cannot be expected to give accurate

**ORIGINAL PAGE IS
OF POOR QUALITY**

simulations of the orogeny. On the other hand, even with such weak faults, only a fraction of the internal deformation is expressed as fault slip; this means that rigid microplate models cannot represent the kinematics either. A universal feature of the better models is that eastern China and southeast Asia flow rapidly eastward (*e.g.*, 20-60 mm/a) with respect to Siberia. The rate of escape is very sensitive to the level of shear traction in the Pacific subduction zones, which is below 6 MPa. Because this flow occurs across a wide range of latitudes, the net eastward escape is greater than the rate of crustal addition in the Himalaya. The crustal budget is balanced by extension and thinning, primarily within the Tibetan plateau and the Baikal rift. The low level of deviatoric stresses in the best models suggests that topographic stress plays a major role in the orogeny; thus, we have to expect that different topography in the past may have been linked with fundamentally different modes of continental collision.

INTRODUCTION

Our zeroth-order understanding of why continental collisions (orogenies) differ from normal oceanic subduction is that continental crust is too buoyant to subduct, and accumulates near the surface in a thick layer which supports high topography and thus changes the patterns of tectonic stress and flow. The beginning of this process in the Himalaya is well dated at about 55 Ma (see chapters by Rowley and Burbank in this volume). Using the known plate motions since this time, the length of the Himalayan arc, and the crustal thickness of India, it is relatively straightforward to compute that about $4 \pm 1 \times 10^5$ km³ of continental crust have been intruded into or subducted under Asia since that time (Le Pichon, Fournier, and Jolivet, 1992). The most basic question one can ask about the

orogeny is, where has this excess crust gone?

Fate of the excess crustal volume

For many years, the debate about this question has emphasized two opposite ideas: that the excess crust was stacked locally beneath Tibet, or was extruded eastward to reduce the area of the Pacific basin.

Growth of Tibet. Since Tibet is the highest and widest plateau on the Earth, and coincides exactly in longitude with the Himalaya, it is clearly a result of the orogeny. Crustal thickness here is about 70 km, or twice that of normal continents. The volume of crust deposited here is uncertain by about a factor of two, depending upon whether the pre-orogenic topography resembled the Altiplano of the Andes, or the low arc of Sumatra. Also, it is very controversial how the crustal thickness was doubled. Emile Argand envisioned a single underthrust of India; this view was recently restated by Powell and Conaghan (1973). A recent variant of this idea is that underthrusting India may have pushed a "pool" of soft lower crust of Asia ahead of it, "inflating" Tibet more uniformly (Zhao and Morgan, 1987; Bird, 1991). Others have argued that underthrusting is minor, and that Tibet has been horizontally shortened to about 50% of its former width (Dewey and Burke, 1973). The idea that Tibet has absorbed most of the surplus crust is supported by a number of plane-stress, thin-plate, finite-strain continuum computer models (*e.g.*, England and McKenzie, 1982; Vilotte, Daignieres, Madariaga, and Zienkiewicz, 1982). When such models are given rigid boundary conditions on all sides, eastward escape is impossible; yet even if escape is permitted by a free eastern boundary, it is never very important in such continuum models (see chapter by Houseman in this volume). In the

homogeneous flat sheet of lithosphere around the model "Tibetan plateau", strain-rates typically decay as a power of distance from the highlands, precluding anything resembling through-going master transform faults. Certain specific heterogeneities (like a rigid Tarim Basin) have been added to some of these models (Vilotte *et al.*, 1984; England and Houseman, 1985) and this causes local perturbations and broad shear zones, but does not change the basic result.

Continental escape. The antithesis in this debate is that China was extruded to the east, overriding and shrinking the Pacific basin. This idea originated in the mapping (from satellite images) of great transform faults such as the Altun Tagh and Red River faults, the linkage of Red River fault slip with the Cenozoic opening of the South China Sea, and a proposed analogy between Asia and a sheet of plastic material deformed in plane-strain (Molnar and Tapponnier, 1975; Tapponnier and Molnar, 1976; 1977). (According to this view, gravity prevents further crustal thickening after an initial transient, so the later phases of the orogeny have minimal strain along vertical axes.) Transform-dominated extrusion tectonics of this style was modeled using strain-weakening plasticines or clays (which form faults spontaneously) with a plane-strain constraint (Tapponnier, Peltzer, Le Dain, and Armijo, 1982; Peltzer and Tapponnier, 1988).

Actually, the debate should be widened to include two other possibilities:

Regional crustal thickening. It is notoriously difficult to determine paleoelevations in the absence of marine sediments, and Cenozoic marine rocks are found only in eastern China. Thus, one cannot rule out distributed crustal thickening in Siberia, Mongolia, and western China by lesser amounts, which might have increased the elevation of Asia by perhaps a kilometer.

Conversion of gabbroic lower crust to eclogite. Many believe that the typical composition of the lower continental crust resembles that of gabbro. If so, then whenever crust is thickened and heated beyond 600-800°C, its lower layers could convert to the rock eclogite, primarily by the growth of garnets and the dissolution of feldspars (Ahrens and Schubert, 1975). This transformation would convert the rock from a "crustal" density of about 3000 kg m⁻³ to a "mantle" density like 3300 kg m⁻³. For tectonic purposes, this volume of material would be subtracted from the crust and added to the mantle. It is impossible to compute a prediction of the size of this effect, because the transition is broad in P/T space, the reaction kinetics are sluggish, and the actual composition of most lower crust is unknown.

Budget for excess crust

In a recent attempt to quantify and account for all of the excess continental crust in this orogeny, Le Pichon *et al.* (1992) showed that crustal thickening (both in Tibet and in the rest of Asia) probably accounted for 60% of the excess volume. This implies that about 40% of the excess volume went either into eclogite or into continental escape. Unfortunately, there is no known way to quantify the production of eclogite, except that it is probably non-negative. This only gives an upper bound (40%), but no lower bound, on the total amount of continental escape during the orogeny. Also, the assumptions behind such calculations are themselves controversial; by using a lower initial elevation for Asia and a greater volume for eroded sediment, Rowley (this volume) reaches a much lower limit (5%) for the amount of continental escape. The uncertainties in such an analysis are quite large.

History of the disposition of excess crust

Can these views be reconciled by postulating that "escape" was the dominant mode during only one interval of the orogeny? Theoretically, one would expect that Tibet rose first, gradually increasing the deviatoric stress on adjacent parts of Asia, until the great transforms broke through and made escape the dominant mode in the latter part of the orogeny. However, Harrison, Copeland, Kidd, and Yin (1992) have reviewed the sedimentologic and metamorphic data and showed that Red River fault activity (the best-documented part of the escape) was essentially completed before the rise of Tibet. In a further complication, Molnar and Tapponnier (1978) documented active normal faulting in Tibet which shows it has actually been collapsing vertically and extending in the East-West direction since the Pliocene, implying that escape should once more be dominant today. However, it is necessary to recall the alternative possibilities of regional crustal thickening or eclogite formation. Hence, there is no easy solution of this kind.

Research plan

Considering how many fine scientists have argued over this problem for two decades, we cannot expect to resolve it with one new argument or computation. Our view is that we should begin by understanding the dynamics (*i.e.*, the kinematics or flow field, and also the balance of forces) in the present, and only then consider how to extrapolate into the past. If at first we only try to model present velocities and stresses, we are freed from the need to choose initial conditions for the shape of Asia, the shape of India, the map of crustal thickness, and the map of heat-flow. Instead, we can work with published maps of present elevation, heat flow, and crustal thickness which are based on actual data

(however sparse). We know the present relative velocities of the surrounding plates with good precision. We can incorporate existing maps of active Quaternary faults, and test whether these planes are major weaknesses, or only passive strain-orientation indicators analogous to "slip lines" in the plastic deformation of metals. Especially, we can benefit from historical data on seismicity, geodesy, and stress directions; these will not be input data to the models, but instead can be compared to predicted outputs, as a test of the relative realism of different models in a set.

One final motivation for beginning with neotectonic studies is that a large fraction of the world's population lives in Asia under the constant threat of devastating earthquakes. Since economic resources are not sufficient to move all of these people into earthquake-resistant housing, some prioritization based on relative risk is clearly needed. A successful neotectonic model could predict the long-term mean slip rates of all the major faults in Asia, which could provide some measure of their relative seismic hazard, until it becomes possible to replace these estimates with the results of local geologic and geodetic studies.

FINITE-ELEMENT MODEL

Assumptions

Spherical planet. We ignore planetary rotation and approximate the lithosphere as a spherical shell (of variable thickness). We assume radial, laterally-homogeneous gravity, so that the sphere is a geoid. (As with mantle-convection theories, our methods can be applied to a real rotating planet by the simple trick of measuring relative radial position with respect to the actual geoid, not with respect to the planet's center.)

Creeping flow. Because we seek to compute velocities which are averaged over a longer time scale than that of the earthquake cycle, we ignore individual earthquakes and all other accelerations except gravity.

Anelastic rheology. In a quasi-steady state with time-invariant boundary conditions, elasticity contributes a negligible fraction of the strain-rate in viscoelastic solutions. The "viscous" part of the strain-rate is caused by thermally-activated dislocation creep and/or frictional sliding on faults, both of which are nonlinear ("non-Newtonian"). We neglect elastic strain entirely to eliminate the need for unknown initial conditions, and for time-steps.

No flexural strength. We assume no vertical shear traction on vertical planes, and that vertical normal stress is therefore lithostatic at all points. (Also, most parts of most models will be designed to be isostatic, but this is not a constraint of the method. If the elevation and density structure taken together would imply anomalous tractions at the base of the model, such tractions will be properly considered in the momentum balance.)

"Thin-plate" (actually, "thin-shell"). The horizontal components of the momentum equation are vertically (radially) integrated through the lithosphere before they are applied as constraints on the solution. In this paper, we shall also assume that the horizontal components of velocity are nearly independent of depth (actually, they are proportional to r). This second assumption is not essential, and Bird (1989) showed how it could be relaxed in the case of flat-Earth models.

Constant thermal properties. We assume constant thermal conductivity and heat productivity in all parts of crust, with (distinct) constant properties in all mantle lithosphere.

Incompressibility (consistent with neglect of elastic strain).

Steady state, vertical heat conduction. The geotherm is assumed to depend only on heat flow and thermal properties. (This assumption can also be relaxed, with additional programming.)

The equations derived from these assumptions are contained in Kong and Bird (in press), together with a report on verification tests of the resulting Fortran77 program (SHELLS). Essentially, we divide the lithosphere into spherical-triangle elements, whose corner points are called nodes. The strength of the lithosphere is determined by 3-D numerical integrals throughout the volume, taking account of different crust and mantle properties, varying geotherms, varying strain-rates, and migration of the brittle/ductile transition(s). The horizontal components of velocity at nodes are the primary unknowns that we solve for. Because the rheologies we use are nonlinear, it is necessary to approximate them with linear ones, and then iterate each computation until the linearized and nonlinear rheologies coincide at all integration points in the grid.

Input Datasets

Grid geometry. The finite element grid used in our simulation experiments is shown in Figure 1. All previous simulations of Asia (whether in the computer or in the lab) have used plane methods. This made it necessary either to move the model boundaries artificially close to Tibet, or to accept geometric distortions near the model edges. In practice, all previous authors have used artificial straight boundaries. We take advantage of the spherical-shell method to use mostly natural plate boundaries for Asia. Along the south margin, we include the Zagros orogen, the Makran oceanic subduction zone, the sinistral transforms of Pakistan,

the Himalayan frontal thrust, the dextral transpressive boundary of Burma, and the Indonesian subduction zone. (In each case, the edge of the grid is a fault element.) On the east, the boundary follows the oceanic subduction zones of the Philippines, Taiwan, Japan, and the Kamchatka arc. In the northeast, we follow the North America/Eurasia boundary proposed by Cook, Fujita, and McMullen, (1986) to the Nansen Ridge. It is only at this point that we depart from actual plate boundaries, to avoid modeling the complex Mediterranean region and the eastern Atlantic. Our model is terminated at the meridian of 40°E (west of the Urals), beyond which the Himalayan orogeny is unlikely to have any influence.

The faults included in the grid include all those indicated as active or potentially active on two tectonic maps of Asia: Institute of Geology (1979) and Ma (1987). We also include a single thrust fault to represent the inactive Ural suture, to see if the stress fields in our models would disturb it. Because it is unlikely that mature faults of large displacement actually terminate without connections, we connect together adjacent faults in places where young sediment may prevent the connection from being mapped. (This connectivity is quite important to preserve the effective degrees of freedom of models in which the faults are weak.)

It is necessary to assume a dip for each fault segment. We first classify all faults tentatively as thrust, normal, or strike-slip based on field data, fault plane solutions, topography, or mechanical intuition. We then assign dips of 25° for thrusts, 65° for normal faults, and 90° for strike-slip faults, consistent with the hypothesis that they initially formed as Mohr-Coulomb shear fractures in a homogeneous medium of friction $f = 0.85$. It is important to realize that the

sense of dip-slip tentatively assigned is not a constraint on the solutions: a fault assigned a dip of 25° may actually slip in a thrust, transpressive, strike-slip, transtensional, or normal sense, depending on the stresses applied to it. Only faults assigned a dip of 90° are constrained to move in a strike-slip sense, either dextral or sinistral. (To avoid artificial locking at a joint between two strike-slip fault elements of different azimuths, their mean azimuth is used to impose this constraint.) Because an incorrect strike-slip constraint could eliminate necessary degrees of freedom from our solutions, we assign a compromise dip of 45° to some faults whose dip and sense of slip are uncertain (*e.g.*, the boundary fault between India and Burma). All faults will lock if there is not enough deviatoric stress in their vicinity.

Elevation. To accurately represent the forces associated with topography, elevations and ocean depths are taken from the ETOPO5 global dataset of 5' means. Then, elevations of nodes are adjusted so that the piecewise-planar topography of the model is best-fit to this data. Finally, the depths of all subduction-zone trenches are corrected by hand, since the process above tends to underestimate them. Accurate trench depths are important so that the lithostatic component of the boundary tractions on the model edges will be correct.

Heat-flow. Unfortunately, there are large parts of Asia with no heat-flow wells, at least in the open literature. Our map of heat-flow (Figure 2) is based on 5° means kindly provided by Henry Pollack (personal communication, 1993), with some finer-scale detail based on maps by Duchkov *et al.* (1985) (Siberia) and Lysak (1992) (Baikal rift). Excluding the area around the spreading Nansen Ridge, this heat-flow model is conservative, ranging only from 52 to 100 mW m⁻². Most of

Tibet and the tectonically active area to the east (as far as 110°E) is represented by a uniform 60-67 mW m⁻².

Lithosphere thickness. We assume that the base of the mantle lithosphere is an isothermal surface at 1300°C, and compute its depth from the heat-flow data, assuming thermal conductivities of 3.5 and 6.0 W m⁻¹ °K⁻¹ in the crust and mantle, respectively, and radioactive heat production of 4.6×10⁻⁷ W m⁻³ in the crust. The thickness of the mantle lithosphere is typically 85-105 km, but values up to 160 km are inferred in the Siberian craton, and smaller values are computed for East Tibet, the Sea of Japan, and in the Baikal rift (Zorin, Kozhevnikov, Novoselova, and Turutanov, 1989).

Crustal thickness. After the computations above, we adjust the crustal thickness to achieve local isostasy everywhere with respect to a typical midocean rise. This computation assumes crust and mantle densities of 2875 and 3330 kg m⁻³, respectively (at 0°K; the corresponding volumetric thermal expansion coefficients are 2.4 and 3.1×10⁻⁵ K⁻¹). The resulting thicknesses range from 5 km (enforced as a minimum) in the ocean basins to 75 km in Tibet, with a modal value of 40 km in Asia. Because of the constraint that crustal thickness is no less than 5 km, a very thin strip of model along each oceanic trench can not be isostatically balanced; it is assumed that the necessary tensional anomaly in the vertical stress at the base of the lithosphere is provided by the dynamics of subduction.

Rheology. All simulations share a common pair of dislocation-creep rheologies (one valid in the crust, and the other in the mantle lithosphere). The equation for creep strength involves principal stresses σ_i (with tension positive), principal strain-rates $\dot{\epsilon}_i$, absolute temperature T , depth z , and four constants (A, B, C, n):

$$\tau(\sigma_3 - \sigma_1) \leq 2A(\dot{\epsilon}_3 - \dot{\epsilon}_1) \left(2\sqrt{-\dot{\epsilon}_1\dot{\epsilon}_2 - \dot{\epsilon}_2\dot{\epsilon}_3 - \dot{\epsilon}_3\dot{\epsilon}_1} \right)^{(1/n-1)} \exp\left(\frac{B+Cz}{T}\right)$$

The crust/mantle values of each constant are: $A = 2.3 \times 10^9 / 5.4 \times 10^4 \text{ Pa s}^{1/n}$; $B = 4,000 / 18,314 \text{ }^\circ\text{K}$; $C = 0 / 0.017 \text{ }^\circ\text{K m}^{-1}$; and $n = 3$. These values were based on previous experience in modeling California (Bird and Kong, 1994) and Alaska (Bird, in press) with similar programs.

At low temperatures, the strength of the lithosphere is limited by frictional sliding. Typical laboratory tests show friction coefficients $f = 0.60$ to 0.85 for a wide variety of rocks. We assume that the continuum blocks between faults have this friction, and that they are pre-fractured on a variety of planes (we ignore cohesion). However, most models assume a lower friction coefficient in fault elements ($f_f \geq 0.04$). All frictional strengths are computed assuming locally hydrostatic pore pressure. If major faults are actually filled with anomalous, near-lithostatic pore pressure, then their true friction coefficients must be higher than the apparent coefficients determined in this study.

The many active subduction zones which ring the model on the southern and eastern sides (including the Himalayan continental subduction zone) are probably different from other thrust faults because of the rapid subduction of sediments and the dynamic maintenance of high internal pore pressures. In previous studies, Bird (1978a) found a maximum mean traction of only 20 MPa in the Himalayan zone, and Bird (1978b) found average shear tractions of only 9-32 MPa in the Tonga and Mariana oceanic subduction zones. To represent this, we have added special programming which monitors the mean shear traction in these boundary subduction zones and prevents these tractions from exceeding a preset limit.

Boundary conditions. Around most of the perimeter of the model the edge of the grid is ringed with fault elements. Therefore the outermost nodes belong to the adjacent plates, and it is these nodes which require boundary conditions. We impose the present velocities of the Arabia, India, Australia, Pacific, and North America plates (with respect to Eurasia) from the NUVEL-1 model of DeMets, Gordon, Argus, and Stein (1990). The present velocities of the Philippine plate are from Seno *et al.*, 1987. The short northern boundary is held fixed in the reference frame of western Eurasia (Europe). Along the artificial western boundary, we permit free slip in the N-S direction, but prevent any E-W velocity component. (This particular boundary location was chosen because it lies along a local mirror plane of symmetry in the orocline of the Zagros orogen. Local symmetry then dictates this choice of boundary conditions.)

Scoring

In order to choose the best model, we compare our modeling results with geologic and geophysical data, such as relative velocities between pairs of points measured by Very Long Baseline Interferometry (VLBI) or Global Positioning System (GPS) geodesy, long-term-average fault slip rates from geological or morphological research, and stress directions.

Maximum horizontal stress directions were compiled by Zoback (1992) for the whole Earth. There are 1,624 measurement points in our model region. In North China, there are many northeast-trending active normal faults, and the maximum horizontal stress (σ_{H1}) directions associated with a known normal-faulting stress regime are mostly NE or ENE, as we would expect. However, some σ_{H1} data of "unknown stress regime" point NW. Therefore, we reject σ_{H1}

directions of "unknown stress regime" as less reliable and use only the 1,033 σ_{h1} directions with known stress regime. From a variogram which we computed using this data, we find that the stress directions contain random errors with standard deviation of 30°. With 30° error, this dataset is not a very reliable scoring reference.

Heki and Koyama (1993) reprocessed the VLBI data of Ryan *et al.* (1993) and found that Shanghai in east China is moving southeastward at 10 mm/a relative the interior of the Eurasia. But Robaudo and Harrison (1993) used combined VLBI and Satellite Laser Ranging (SLR) data and got the opposite result for the same station, that Shanghai is moving northwestward at 10 ± 2 mm/a with respect to Eurasia. Unfortunately, Shanghai is the only station in Eurasia that is east of the Urals. At the present time, we cannot tell which of above two opposing conclusions is correct. So, we will not this datum in scoring our results. However, our model results will be able to tell which is most reasonable in terms of fitting with other data sets.

Only a very few major faults in Asia have known slip rates. We use the slip rates of 13 major faults (Table 1) to score our model results in a second way. One common problem with published geologic slip rates is that it was difficult to determine the age of the offset feature. Some ages are merely assumed (*e.g.*, Peltzer, Tapponier, Gaudemer, and Meyer, 1988; Peltzer, Tapponier, and Armijo, 1989). Another consideration in using these data is that the faults in our model represent fault zones, not individual faults; but the published geologic slip rates are often for individual faults. Other published slip rates (Ma, 1987) were determined from sums of seismic moments, and it is questionable whether these

short-term rates can represent the long-term average activity of the faults. It almost seems that there is no reliable data we can use to test our modeling results.

However, for most faults in Asia, we know their motion senses, that is, relative movement directions. Although the slip rates of some major faults are controversial, there are few questions about their motion senses. We compile a dataset of fault motion senses for 19 major faults in Asia (Table 2), and use this to compute a third kind of score.

Considering the problems of above data sets, we will give greater weight to fault motion sense than to the other data sets in choosing the best models.

Experiments

The first set of models is to test if the friction coefficient on faults in Asia is as small as that in southern California (Bird and Kong, 1994) and Alaska (Bird, in press). In this set of models, there is no shear traction limit on the subduction zones, which are treated like any other fault element. The internal friction coefficient of the blocks between faults is kept at 0.85. We calculate models with fault friction coefficients (f_f) of 0.085, 0.17, 0.51 and 0.85. Table 3 gives the scores of these 4 models. The errors of fault slip rate and stress direction hardly vary. The percentage of faults with the correct movement sense declines with each increase of fault friction. At f_f larger than 0.51, almost all faults are inactive (Figure 3). When f_f is small (0.17 to 0.085), many faults are active (Figure 4) and about 60% of the predicted fault slip directions match the sense data. At f_f equals 0.085, the velocity of Shanghai (relative to Eurasia) is close to the geodetic result of Robaudo and Harrison (1993). The results of this set of models show that the major faults of Asia have low friction coefficient, as in southern

California and Alaska. However, the best model still has important defects. Many major faults are still not moving or move in the wrong direction. For example, the Baikal rift and Shanxi graben are supposed to be normal faults but in Model J9401 both of them are thrusting (Figure 4). The Urals, which should be inactive, are thrusting slowly. All of these errors probably result from too much E-W compression, caused by too much shear traction on the Pacific subduction margin. The Altun Tagh fault is not as active as it should be. And, slip rates along the plate boundaries with the India and Australia plates are probably too small. Obviously, even the best model in this group is not satisfactory.

Bird (1978a) concluded that the mean shear traction along the Main Boundary Thrust between the India plate and Eurasia plates should not be larger than 20 MPa. The slow slip of this fault in model J9401 (6-7 mm/a) also implies that we are overestimating the strength of this fault. For our next set of experiments, we test the effects of varying the traction on the interplate surfaces of subduction zones. We will treat the boundary thrust faults as a special kind of fault on which shear traction will be limited to a preset value. This value will be an input parameter that can be adjusted to fit the scoring datasets. We vary this parameter (T) from 30 down to 5 MPa. When it is more than 20 MPa, the Main Boundary thrust hardly moves. From seismic moments, one can infer about 36 mm/a slip rate on this fault (Ma, 1987). Jackson and Bilham (1993) used relative uplift rates of 6 ± 2 mm/a in the Himalaya to infer a convergence rate of about 10 mm/a for the ramp portion of the boundary thrust. Although there is controversy about the slip rate of the Himalayan boundary, we are sure that the Main Boundary thrust is quite active. If we take the numbers above as the range of the

slip rate of the Main Boundary thrust, the slip rate should be 10 to 36 mm/a. When T equals 15 MPa, the slip rates along the Main Boundary fault fall within this range. When this parameter is less than 10 MPa, the Tibetan plateau completely collapses along its southern edge (Figure 5). A shear traction of 15 MPa along the Main Boundary Thrust is probably a reasonable estimate, and we will use this value for our following calculations.

However, the fault motions inside the Asian continent is still not right. The major faults on the eastern side of the Tibetan plateau are not moving. The Altun Tagh is too slower and Baikal is almost a purely strike-slip fault. To improve our modeling results our next step is to test possible differences in traction between the Main Boundary Thrust and the oceanic subduction zones. We will use two parameters to adjust the traction on subduction zone surfaces. One is for the traction on the Main Boundary Thrust; we call it the Himalayan subduction traction (T_H). The other is for all other subduction zone and is called the oceanic subduction traction (T_O). We assign different values for both T_H and T_O ranging from 1 to 20 MPa. No matter how T_O changes, as mentioned above, the slip rates of the Main Boundary thrust are always within the range of 4 to 36 mm/a when T_H is between 13 and 17 MPa, with an ideal value of 15 MPa. (And, as we will see later, with T_H equal to 15 MPa we can get better scoring results.) When T_O equals 2 to 4 MPa, we get the best scoring results for both slip rate and fault motion sense (Table 4).

These scores of slip rate and fault motion data favor low shear traction on the oceanic subduction zones. But the stress direction errors are large (40°) in each model. We do not consider this a serious problem. Even if our modeling

results were only a few degrees different from the true stress direction, the stress dataset has 30° standard deviation, so it must be expected that the mismatch of model to data would be more than 30° . Stress is apparently not well enough known to discriminate between models.

Our best model has parameters: Himalayan traction $T_H = 15$ MPa, oceanic traction $T_O = 2$ MPa, fault friction $f_f = 0.065$, and block friction = 0.85. This model also predicts a velocity at Shanghai, China close to that of Ryan *et al.* (1993) and Heki and Koyama (1993).

Figure 6 shows our predicted velocity field in Asia. Material is moving away from the Tibetan plateau toward the eastern boundary of Asia. This result shows that material is currently "extruding" from the Himalayan orogen. This eastward motion is mainly to the SE of a line from the Pamirs to Baikal. On the NW side of this line the crust is very stable. This extrusion is distributed over almost the whole of central and east Asia, and is not the result of rigid block motion. A major extrusion boundary lies along the Tian Shan, instead of at the Altun Tagh fault.

Unfortunately, we do not know when this kind of extrusion started, whether at the collision between India and Asia, or after the initial rise of Tibet, or only after the postulated delamination of Tibet in the Pliocene. Our modeling cannot address such historical questions until palinspastic maps of paleotopography and fault networks have been drafted.

Figure 7 shows our predictions of long-term average fault slip rates. Our sense predictions are correct for most major faults in Asia; the Baikal rift is opening, and the Altun Tagh, Red River, and South and North Tian Shan faults

are moving in the correct direction. Our prediction of the Altun Tagh fault rate (2-8 mm/a) is much smaller than that of Peltzer *et al.* (1989), but is almost the same as that determined from offset paleo-stream-channels with ^{14}C ages (Altun Tagh Active Fault Research Group, 1992). Based on a lot of field work, they found the dextral slip rate of the Altun Tagh fault is 4.3 to 5.2 mm/a, and the vertical slip rate is a minimal 0.3 to 0.8 mm/a. If it is true that Altun Tagh fault does not move very fast, our prediction would be that the boundary of the extruding material lies along the Tian Shan.

In this model the normal faults representing the Baikal rift slips at up to 35 mm/a, implying up to 15 mm/a of spreading. (Note: To convert from dip-slip rates to discontinuities in horizontal velocity, reduce thrusting rates by 9% and normal-faulting rates by 58%.) This is almost equal to the relative velocity of the surrounding blocks, which is about 18 mm/a. Thus, the model suggests that the rifting is primarily "passive" (driven by microplate motions) rather than "active" (driven by local density anomalies). The main role of the thin lithosphere and high heat-flow in the Baikal rift is to cause the spreading to concentrate there, whereas to the SW it is very diffuse (Figure 8).

One big problem with our results is that the Xianshui He fault and the Longman Shan thrust are not moving. This might result from the low resolution of our model, especially the very smooth heat flow field which we used (Figure 2). In the region of these faults, almost no heat flow data is available. So heat flow is uniform across these faults in our model, and the rheology (which is dependent on the geotherm) is uniform. Perhaps some special local weakness is required to facilitate the slumping of crust down the eastern margin of Tibet.

Because of this failure in our prediction, at this stage our model is not yet ready to estimate the seismic hazard distribution within Asia.

Figure 8 shows the predicted principle strain-rates within the continuum blocks (ignoring slip on fault elements). This can be interpreted as the deformation due to all faults too small to appear in our grid. The deformation is almost all tensional or transtensional and is concentrated in the Tibetan plateau and its the neighboring Baikal rift and Ordos plateau. (There is thrusting in this model, but it occurs in fault elements where we have lowered the friction, not as distributed deformation in the stronger blocks.) The Tarim basin and southeast China are stable.

The vertically integrated stress anomalies are shown in Figure 9. The quantity displayed is the vertical integral through the lithosphere of the stress anomaly (relative to the center of a midocean rise). The vertical component of the integrated stress anomaly is dominant in the Tibetan and Ordos plateaus. In the Tian Shan and other areas near to Tibet the maximum compressional components are in directions radiating from the plateau. The distribution of the stresses means that the weight of the plateau is very important in driving the neotectonics of Asia.

CONCLUSIONS

Unfortunately, even the best of our models still fail to reproduce the right direction of slip on a few (11% of) active faults. In other cases, the sense is correct but the rate errors are large. Thus, it would be premature to use these models for seismic hazard estimation in Asia. To achieve major improvements will require more data, of which the most important would be additional heat-flow values for input to the models, and additional geologic slip-rates or geodetic

velocities for testing of the output.

Even at this early stage, it is apparent that the faults of Asia share the anomalous weakness that was previously found in California and in Alaska. Previous continuum finite-strain simulations of this orogeny with finite elements have been based on an implicit assumption that faults are passive strain markers, but not important heterogeneities; this seems to be wrong. Since rapid fault slip implies local concentrations of straining in the ductile part of the lithosphere, there must be a compensating weakness in the frictional part of the fault, with respect to adjacent blocks. The contrasts that we find are too great to ascribe to variations in lithology. More likely, they are due to concentrations of pore pressure along faults, where previously subducted water may be returning to the surface.

The thrust faults of the marginal subduction zones are even more profound heterogeneities: in our model, the best strengths are 15 MPa for the Himalayan thrust, and about 2 MPa for the oceanic subduction zones. Such low strength almost certainly requires near-lithostatic pore pressure in the subducting sediments. The pore pressure may actually equal the minimum compressive stress (σ_3) in these zones, and water may escape by hydrofracturing. Or, pressure may be self-regulating, by a mechanism in which permeability increases exponentially as pore pressure approaches σ_3 . In the latter case, it would be natural for the equilibrium pore pressure (and thus the fault strength) to depend on the permeability of the subducted sediment. The strength difference we infer between the continental and oceanic subduction zones might be explained by the porosity difference between sandstones and abyssal cherts, for example.

An approach to neotectonics that geologists often use is the geometric construction of microplate kinematic models, in which all the deformation is expressed as fault slip (*e.g.*, Bird and Rosenstock, 1984). If our results are correct, then this approach to Asia is also faulty. We find that only a fraction of the extrusion in our best models can be accounted for by slip on fault elements; much more results from distributed transtensional straining of the blocks between. To date, the only modeling method that seems capable of including weak faults, distributed strain, and also finite strain is the laboratory deformation of scaled clay-cakes and other strain-weakening materials.

Our contribution to the debate about the historical importance of eastward extrusion in the Himalayan orogeny is a clear result that it is very rapid today. We cannot state a precise rate because in our models this is sensitive to changes of as little as 1 MPa in the shear traction of oceanic subduction zones along the Pacific margin. However, it is clear that all the best models show rapid extrusion, and that the rate of crustal escape to the east currently exceeds the rate of resupply along the Himalaya. The budget is balanced by distributed crustal thinning and extension, which quantitatively exceeds the internal shortening by thrusting in the Pamires and Tian Shan.

Because of the weak subduction boundaries and weak internal faults, the stresses are quite low in our preferred models of Asia (Figure 9). There are only a few places where the vertically integrated difference between principal stresses exceeds 1×10^{13} N/m (*i.e.*, 100 MPa \times 100 km). Therefore, the regional stress field is naturally dominated by the compression radiating to Tibet, whose gravity-density moment is of comparable size. The present topography largely determines

the stress field, which determines the strain patterns and thus the evolution of topography. The conclusion that we draw from this is that the solution was probably very different (and extrusion much less important) in previous times when the plateau was not so high.

ACKNOWLEDGEMENT

This research was supported by the National Aeronautics and Space Administration, under NASA grant NAGW-3042 to the University of California. All opinions, expressed or implied, are those of the authors, and do not necessarily reflect the position of the U.S. government.

REFERENCES CITED

- Ahrens, T. J., and Schubert, G. 1975. Gabbro-eclogite reaction rate and its geophysical significance. Rev. Geophys. 13: 383-400.
- Allen, C. R., Gillespie, A. R., Han, Y., Sieh, K. E., Zhang, B., and Zhu, C. 1984. Red River and associated faults, Yunnan Province, China: Quaternary geology, slip rates, and seismic hazard. Geol. Soc. Amer. Bull. 95: 686-700.
- Allen, C. R., Luo Z., Qian H., Wen X., Zhou H., and Huang W. 1991. Field study of a highly active fault zone: the Xianshuihe fault of southwest China. Geol. Soc. Am. Bull. 103: 1178-99.
- Altun Tagh Active Fault Research Group. 1992. Altun Tagh active fault zone (in Chinese). Beijing: Seismological Publishing House.

- Avouac, J., and Peltzer, G. 1993. Active tectonics in southern Xingjiang, China: Analysis of terrace riser and normal fault scarp degradation along the Hotan-Qira fault system. J. Geophys. Res. 98: 21,773-807.
- Bird, P. 1978a. Initiation of intracontinental subduction in the Himalaya. J. Geophys. Res. 83: 4975-87.
- Bird, P. 1978b. Stress and temperature in subduction shear zones: Tonga and Mariana. Geophys. J. R. Astron. Soc. 55: 411-34.
- Bird, P. 1989. New finite element techniques for modeling deformation histories of continents with stratified temperature-dependent rheologies. J. Geophys. Res. 94: 3967-90.
- Bird, P. 1991. Lateral extrusion of lower crust from under high topography, in the isostatic limit. J. Geophys. Res. 96: 10,275-86.
- Bird, P. in press. Computer simulations of Alaskan neotectonics. Tectonics in press.
- Bird, P., and Kong, X. 1994. Computer simulations of California tectonics confirm very low strength of major faults. Geol. Soc. Am. Bull. 106: 159-74.
- Bird, P. and Kong, X. in press. A finite element method for modeling tectonic deformation and fault motion on spherical planets. J. Geophys. Res. in press.
- Bird, P., and Rosenstock, R. 1984. Kinematics of present crust and mantle flow in southern California. Geol. Soc. Am. Bull. 95: 946-57.
- Chen, R., and Li, P. 1988. Slip rates and earthquake recurrence intervals of the western branch of the Xiaojiang fault zone (in Chinese). Seismology and Geology 10: 1-13.

- Cook, D. B., Fujita, K., and McMullen, C. A. 1986. Present-day plate interactions in northeast Asia; North America, Eurasian, and Okhotsk plates. J. Geodynamics 6: 33-51.
- DeMets, C., Gordon, R. G., Argus, D. F., and Stein, S. 1990. Current plate motions. Geophys. J. Int. 101: 425-78.
- Dewey, J. F., and Burke, K. C. A. 1973. Tibetan, Variscan, and Precambrian basement reactivation: products of continental collision. J. Geol. 81: 683-92.
- Duchkov, A. D., *et alia*. 1985. Temperature of the lithosphere of Siberia according to geothermal data. Soviet Geology and Geophysics 26: 53-61.
- England, P. C., and Houseman, G. A. 1985. The influence of lithosphere strength heterogeneities on the tectonics of Tibet and surrounding regions. Nature (London) Phys. Sci. 315: 297-301.
- England, P., and McKenzie, D. 1982. A thin viscous sheet model for continental deformation. Geophys. J. R. Astron. Soc. 70: 292-321.
- Harrison, T. M., Copeland, P., Kidd, W. S. F., and Yin, A. 1992. Raising Tibet. Science 255: 1663-70.
- Heki, K., and Koyama, Y. 1993. Lateral extrusion in the Indian-Asian continental collision: an evidence from Very Long Baseline Interferometry (abstract). Eos Trans. AGU 74: Fall Meeting Suppl., 191.
- Institute of Geology. 1979. Seismotectonic map of Asia and Europe. Beijing: Cartographic Publishing House.
- Jackson, M., and Bilham, R. 1993. Interseismic slip-rate and thrust geometry beneath the Nepal Himalaya (abstract). Eos Trans. AGU 74: Fall Meeting Suppl., 68.

- Le Pichon, X., Fournier, M., and Jolivet, L. 1992. Kinematics, topography, shortening, and extrusion in the India-Eurasia collision. Tectonophysics 11: 1085-98.
- Lysak, S. V. 1992. Heat flow variations in continental rifts. Tectonophysics 208: 309-23.
- Ma, X. 1987. Lithospheric dynamics map of China and adjacent seas, 1:4,000,000 (with explanatory notes). Beijing: Geological Publishing House.
- Molnar, P., and Tapponnier, P. 1975. Cenozoic tectonics of Asia: Effects of a continental collision. Science 189: 419-26.
- Molnar, P., and Tapponnier, P. 1978. Active tectonics of Tibet. J. Geophys. Res. 83: 5361-75.
- Peltzer, G., and Tapponnier, P. 1988. Formation and evolution of strike-slip faults, rifts, and basins during the India-Asia collision: An experimental approach. J. Geophys. Res. 93: 15,085-117.
- Peltzer, G., Tapponnier, P., and Armijo, R. 1989. Magnitude of late Quaternary left-lateral displacements along the north edge of Tibet. Science 246: 1285.
- Peltzer, G., Tapponnier, P., Gaudemer, Y., and Meyer, B. 1988. Offsets of late Quaternary morphology, rate of slip, and recurrence of large earthquakes on the Chang Ma fault (Gansu, China). J. Geophys. Res. 93: 7793-812.
- Powell, C. McA., and Conaghan, P. J. 1973. Plate tectonics and the Himalayas. Earth Planet. Sci. Lett. 20: 1-12.

- Robaudo, S., and Harrison, C. G. A. 1993. Plate tectonics from SLR and VLBI - global data. In: Contributions of Space Geodesy to Geodynamics: Crustal Dynamics, ed. D. E. Smith and D. L. Turcotte., pp. 51-71. Washington: American Geophysical Union.
- Ryan, J. W., Clark, T. A., Ma, C., Gordon, D., Caprette, D. S., and Himwich, W. E. 1993. Global scale tectonic plate motions measured with CDP VLBI data, In: Contributions of Space Geodesy to Geodynamics: Crustal Dynamics, ed. D. E. Smith and D. L. Turcotte, pp. 37-49. Washington: American Geophysical Union.
- Seno, T., Moriyama, T., Stein, S., Woods, D. F., DeMets, C., Argus, D., and Gordon, R. 1987. Redetermination of the Philippine Sea plate motion (abstract). Eos Trans. AGU 68: Fall Meeting Suppl., 1474.
- Tapponnier, P., and Molnar, P. 1976. Slip-line field theory as a quantitative method for understanding large-scale continental tectonics. Nature (London) 264: 319-24.
- Tapponnier, P., and Molnar, P. 1977. Active faulting and tectonics in Asia. J. Geophys. Res. 82: 2905-30.
- Tapponnier, P., Peltzer, G., Le Dain, A. Y., and Armijo, R. 1982. Propagating extrusion tectonics of Asia: New insights from simple experiments with plasticine. Geology 10: 611-6.
- Vilotte, J. P., Daignieres, M., and Madariaga, R. 1982. Numerical modeling of intraplate deformation: Simple mechanical models of continental collision. J. Geophys. Res. 87: 10709-28.

- Vilotte, J. P., Daignieres, M., Madariaga, R., and Zienkiewicz, O. C. 1984. The role of a heterogeneous inclusion during continental collision. Phys. Earth Planet. Int. 36: 236-59.
- Zhang P., Burchfiel, B. C., Molnar, P., Zhang W., Jiao D., Deng Q., Wang Y., Royden, L., and Song F. 1991. Amount and style of late Cenozoic deformation in the Liupan Shan area, Ningxia autonomous region, China. Tectonics 10: 1111-29.
- Zhao, W.-L., and Morgan, W. J. 1987. Injection of Indian lower crust into Tibetan lower crust: A two-dimensional finite element model study. Tectonics 6: 489-504.
- Zoback, M. L. 1992. First- and second-order patterns of stress in the lithosphere: The world stress map project. J. Geophys. Res. 97: 11,703-28.
- Zorin, Y. A., Kozhevnikov, V. M., Novoselova, M. R., and Turutanov, E. K. 1989. Thickness of the lithosphere beneath the Baikal rift zone and adjacent regions. Tectonophysics 168: 327-37.

Table 1. Slip rates of some major faults in Asia

Fault	Strike-slip rate (mm/a; dextral positive)		Relative vertical rate (mm/a, thrust positive)		Reference
	Minimum	Maximum	Minimum	Maximum	
Altay	4.6	10	0.2	1.3	Ma, 1987
Altun Tagh	-30	-4.3			Peltzer <i>et al.</i> , 1989; Altun Tagh Active Fault Research Group, 1992
E. West Kunlun			1.5	7.5	Ma, 1987; Avouac and Peltzer, 1993
Haiyan	-10	-5	0.5	0.8	Ma, 1987
Qilian Shan	-7.7	-3	0.4	1.9	Ma, 1987; Peltzer <i>et al.</i> , 1988; Zhang <i>et al.</i> , 1991
Red River	2	5			Allen <i>et al.</i> , 1984
Shanxi	0.5	2		-0.5	Ma, 1987
Tanlu	1	2			Ma, 1987
W. West Kunlun	10	25	0.5		Ma, 1987
Weihe	-6	-2			Ma, 1987
Xianshui He	-20	-10			Allen <i>et al.</i> , 1991; Ma 1987
Xiaojiang	-7	-4.6			Chen and Li, 1988; Ma 1987
Yinchuan	3	7	-1.0	-0.5	Ma, 1987

Table 2. The motion senses of some major faults in Asia
(from Ma, 1987; Institute of Geology, 1979)

Fault	Strike-slip (D = dextral, S= sinistral)	Dip-slip (T = thrust, N = normal)
Afghanistan-Turkey	D	T
Altay	D	
Altun Tagh	S	
Baikal	S	N
Heto	S	N
Longman Shan	D	T
North Tian Shan		T
Qilian Shan	S	T
Red River	D	N
Sagaing	D	
Shanxi	D	N
South Tian Shan	S	T
Tanlu	D	T
Weihe	S	N
West Kunlun	D	T
Xianshui He	S	
Xiaojiang	S	T
Yinchuan	D	N
Ural	locked	locked

Table 3. Scores of models with different fault friction

Model	Fault friction coefficient f_f	RMS prediction error of fault slip rate (mm/a)	Percentage of fault slip senses matching data	Average prediction error of stress direction
J9401	0.085	4.31	63.9%	39.0°
J9402	0.170	4.15	59.6%	38.8°
J9403	0.510	3.96	48.7%	38.7°
J9404	0.850	3.99	42.4%	38.6°

Table 4. Effects of varying shear traction of oceanic subduction

 (T_O) with $T_H = 15$ MPa

Model	Oceanic shear traction (T_O), MPa	RMS Prediction error of fault slip rate (mm/a)	Percentage of fault motion sense which match data	Average prediction error of stress direction
I9401	2	3.04	88.6%	39.7°
I9402	4	3.32	88.6%	39.3°
I9403	6	3.48	84.8%	39.7°
I9404	8	3.60	77.8%	40.3°
I9405	10	3.72	75.3%	40.0°

FIGURE CAPTIONS

Figure 1. Finite element grid used for all neotectonic models. (As in all figures, a stereographic projection of data on the sphere of the Earth.) Solid lines are fault elements, with different tic marks to indicate dip: none = 90°, straight = 65°, box = 45°, triangle = 25°. Dashed lines are boundaries of continuum elements; these have no mechanical significance, but are shown to indicate resolution. The model domain is the entire Asian lithosphere, or all of the Eurasia plate east of 40°E. (A small corner of the Indian plate in the Assam syntaxis is also included because seismicity suggests that this area is deforming.)

Figure 2. Assumed distribution of heat-flow, used to compute lithosphere thickness and strength. The unshaded contours above 120 mW m⁻² are only used along the Nansen Ridge. Most of the tectonically active region is modeled with heat-flow of 60-70 mW m⁻². References in text.

Figure 3. Fault slip rates from an unsuccessful model (J9403), in which the fault friction is too high ($f_f = 0.51$). Locked faults are dashed (except that all boundary faults are solid even if locked). Active faults are labeled with the relative slip rate in the fault plane, in mm/a. (To find the discontinuity in horizontal velocity, reduce thrusting rates by 9%, and normal-faulting rates by 58%.) Very small arrows in hanging walls show the directions of slip. In this model the Himalayan thrusts would be inactive, as well as the Indonesian subduction zone and the Altun Tagh fault. Relative plate motion would be expressed entirely as distributed permanent straining.

Figure 4. Fault slip rates of a more successful model (J9401). Conventions as in Figure 3. Relative to the model in Figure 3, the fault friction f_f has been reduced

to 0.085. This causes all important faults to become active, although many move too slowly. Excessive E-W compression from the Pacific subduction zone margin causes thrusting in the Urals and in the Baikal rift and in Shanxi, all of which are incorrect.

Figure 5. Close-up of predicted velocities in the Himalayan/Tibetan region, from a model (F9402) which fails because the assumed shear traction on the Himalayan thrusts is too low (10 MPa). The eastern front of the Himalaya collapses in a great landslide traveling over 250 mm/a south with respect to Eurasia (or 300 mm/a with respect to India).

Figure 6. Predicted velocities of the best model found to date (K9401). This model has friction of $f_f = 0.065$ in faults but 0.85 in intervening blocks, with shear tractions of 15 MPa in the Himalaya and 2 MPa in the Pacific margin. Note the eastward extrusion of much of China at about 40 mm/a. (This rate is very sensitive to the level of oceanic subduction traction, but the pattern is not.)

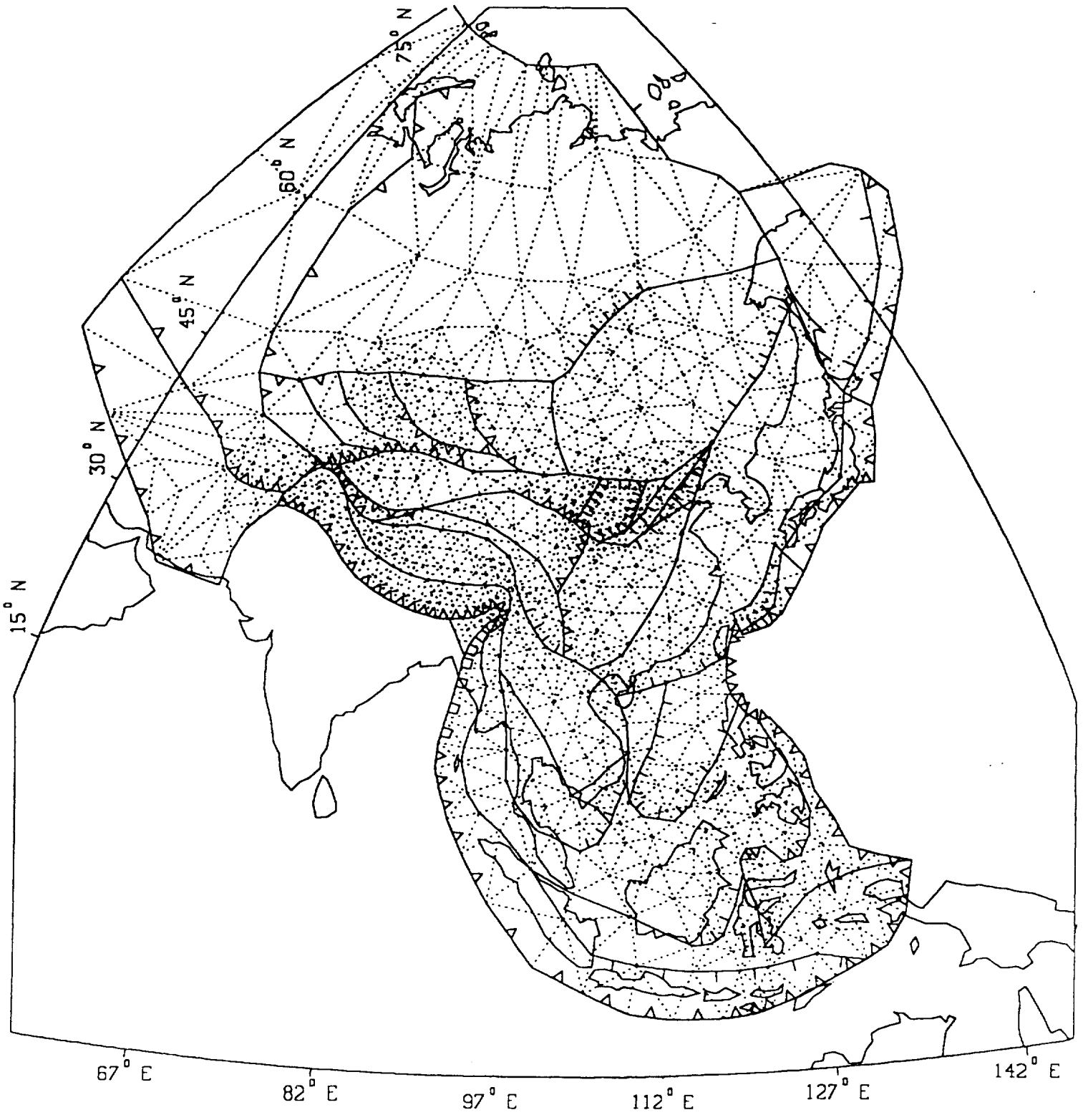
Figure 7. Fault slip rates from the model of Figure 6. Conventions as in Figure 3. Note 19-44 mm/a of horizontal convergence at the Himalayan front, 2-8 mm/a dextral slip on the Altun Tagh fault, up to 13 mm/a convergence in the Tian Shan and 18-27 mm/a in the Pamirs, up to 15 mm/a of divergence at the Baikal rift, and 1-3 mm/a of transtensional faulting in Shanxi. Because of distributed deformation, these slip rates are not compatible with a rigid microplate description of the orogeny.

Figure 8. Close-up detail of distributed straining (excluding faults) from the model of Figures 6-7. The strain-rate tensor is expressed in terms of equivalent faults. The many rectangular symbols indicate grabens. The "X" overprinted on

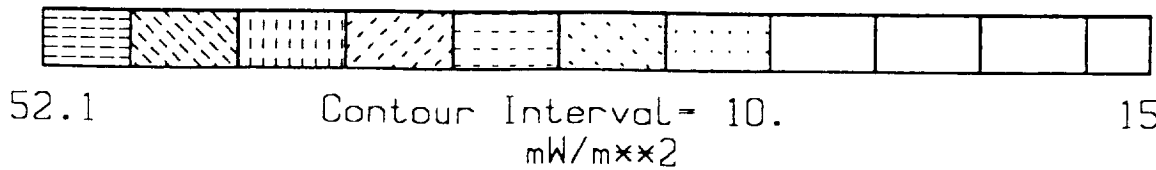
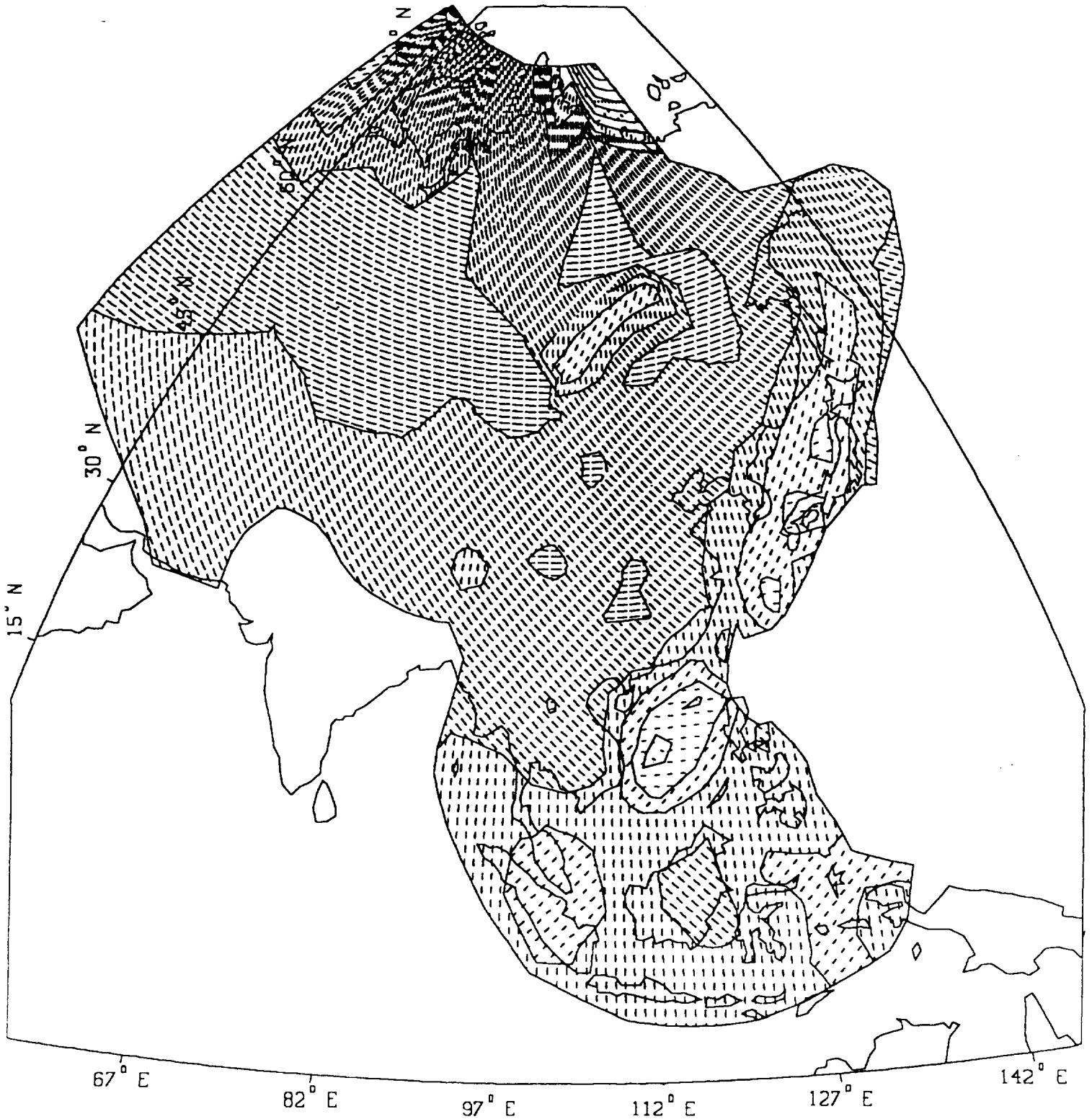
some indicated a component of strike-slip faulting, with the extension axis in the obtuse angle. While this model does include thrust faulting, it usually occurs on weak fault elements (see Figure 7) and not in the stronger intervening blocks (shown here). The only exception is some distributed thrusting (dumbbell symbol) in the Hindu Kush.

Figure 9. Vertically-integrated (through the lithosphere) stress anomaly (with respect to a midocean rise) tensors from the model of Figures 6-8. Circles indicate a compressive component along the vertical axis, and are proportional to the gravity/density moment (almost proportional to topography). In weak areas like Tibet, the horizontal components tend to become equal, causing horizontal compression to radiate through the lowlands around Tibet.

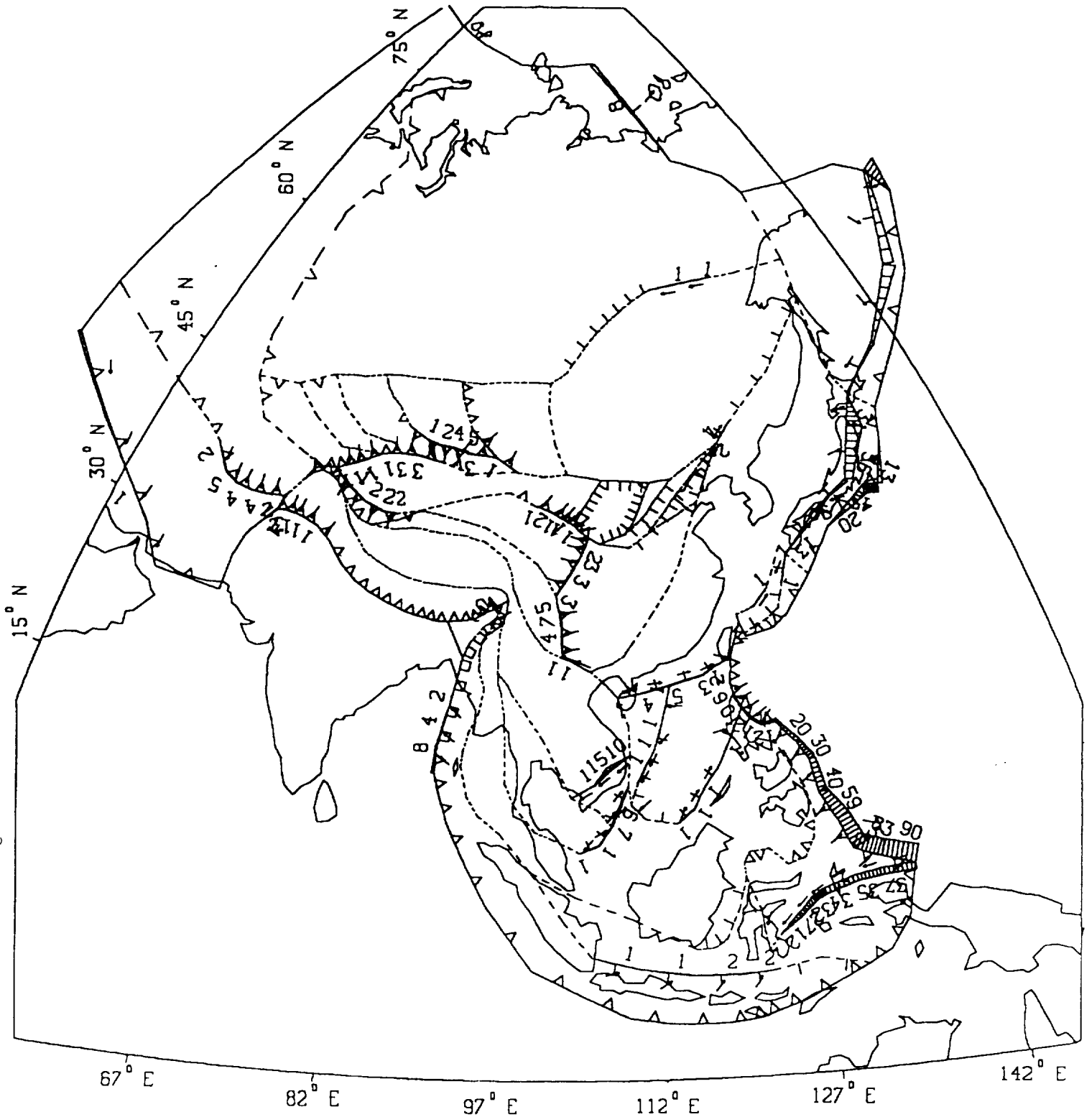
FINITE ELEMENT GRID
ASIA 9413(7/94; LIMITED TRACTION ON INDIAN SUBDUCTION ZONE



HEAT-FLOW
ASIA 9413(7/94; LIMITED TRACTION ON INDIAN SUBDUCTION ZONE



MEAN SLIP-RATE OF FAULTS
 ASIAJ9403: FAULTS 0.51 , NO TRACTION LIMIT ON SUBDUCTION ZO



SLIP-RATE :

5

mm/year

LOCKED

DEXTRAL

←

SINISTRAL

→

THRUST

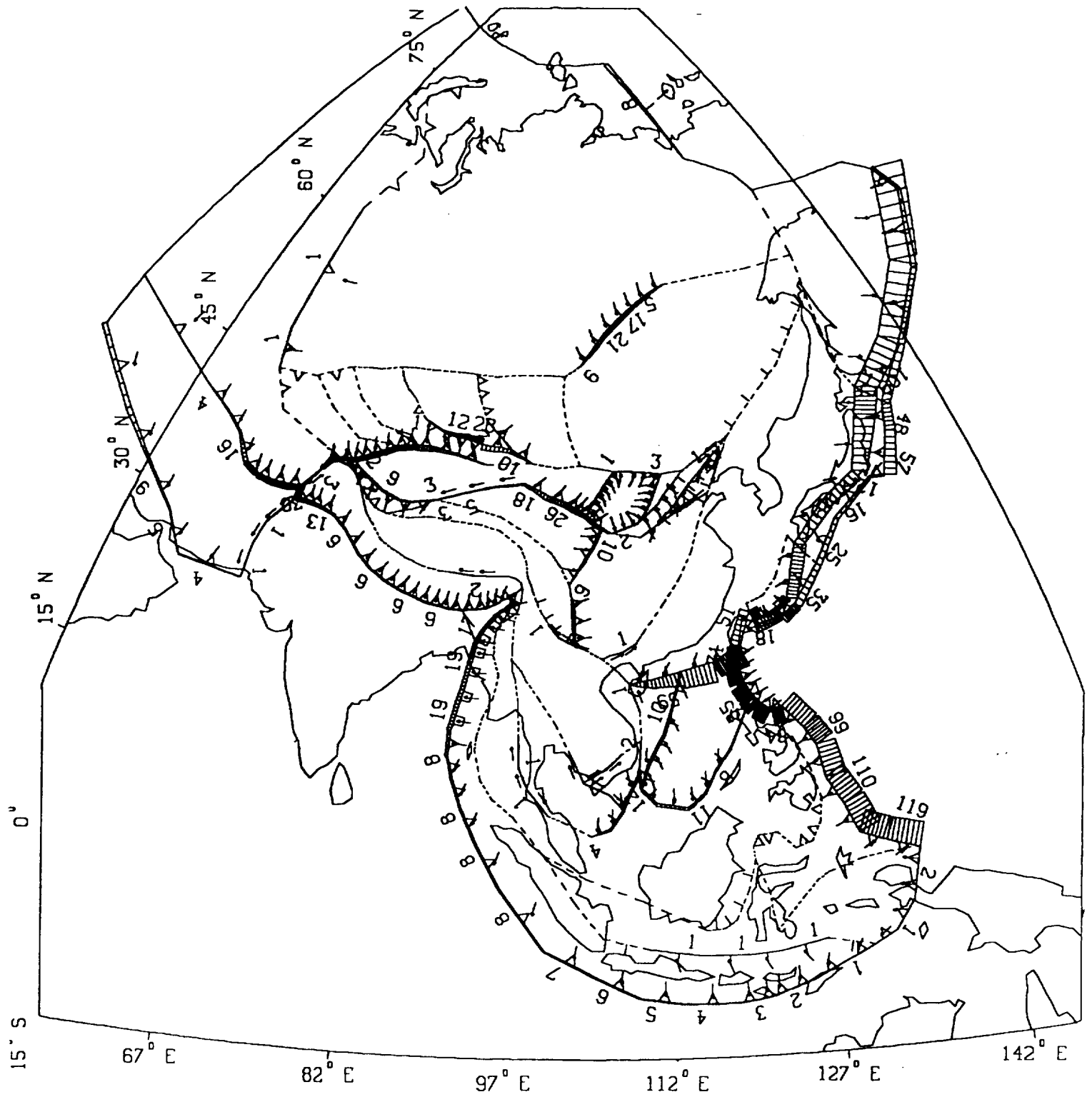
↑

NORMAL

↓


(3)

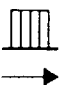
MEAN SLIP-RATE OF FAULTS
 ASIAJ9401: FAULTS 0.085 , NO TRACTION LIMIT ON SUBDUCTION ZONE




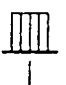
SLIP-RATE: 5
 mm/year

LOCKED: - - - - -

DEXTRAL: 

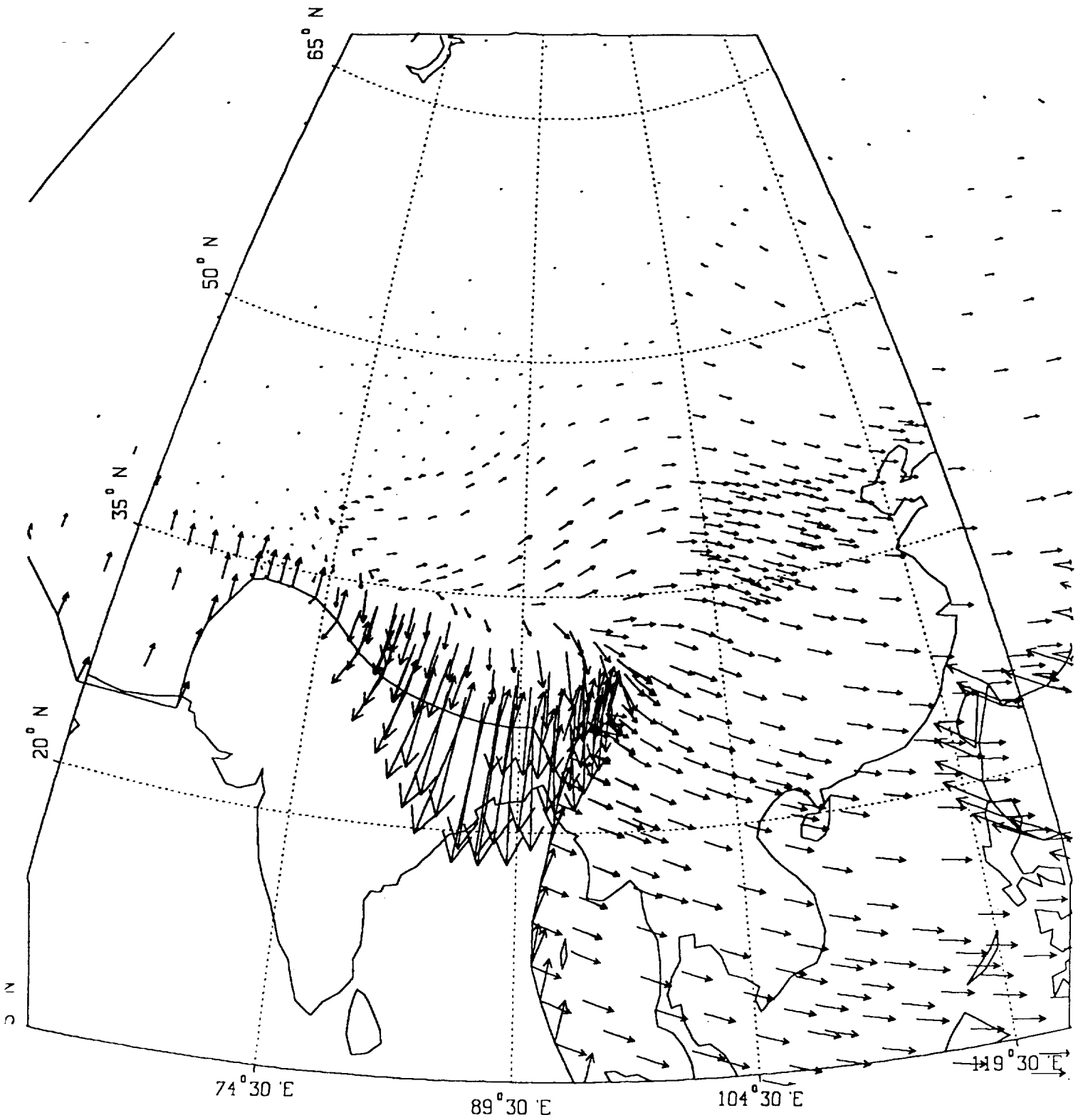
SINISTRAL: 

THRUST: 

NORMAL: 

(4)

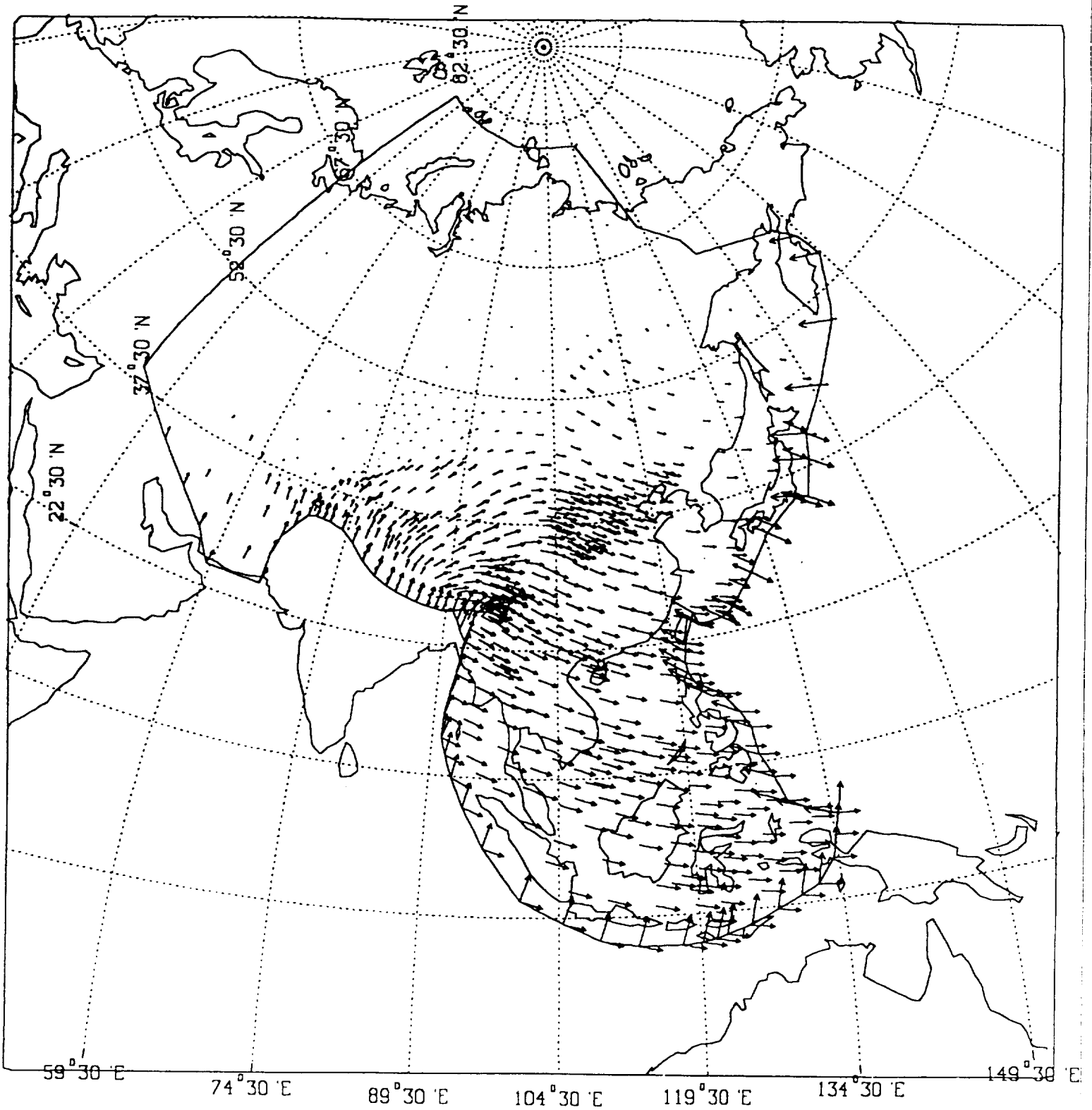
SURFACE VELOCITY
ASIAF9402: FAULTS 0.085 , SBDCT 10 AND 2 MPA, BLOCK 0.85



→ 73.7 mm/year

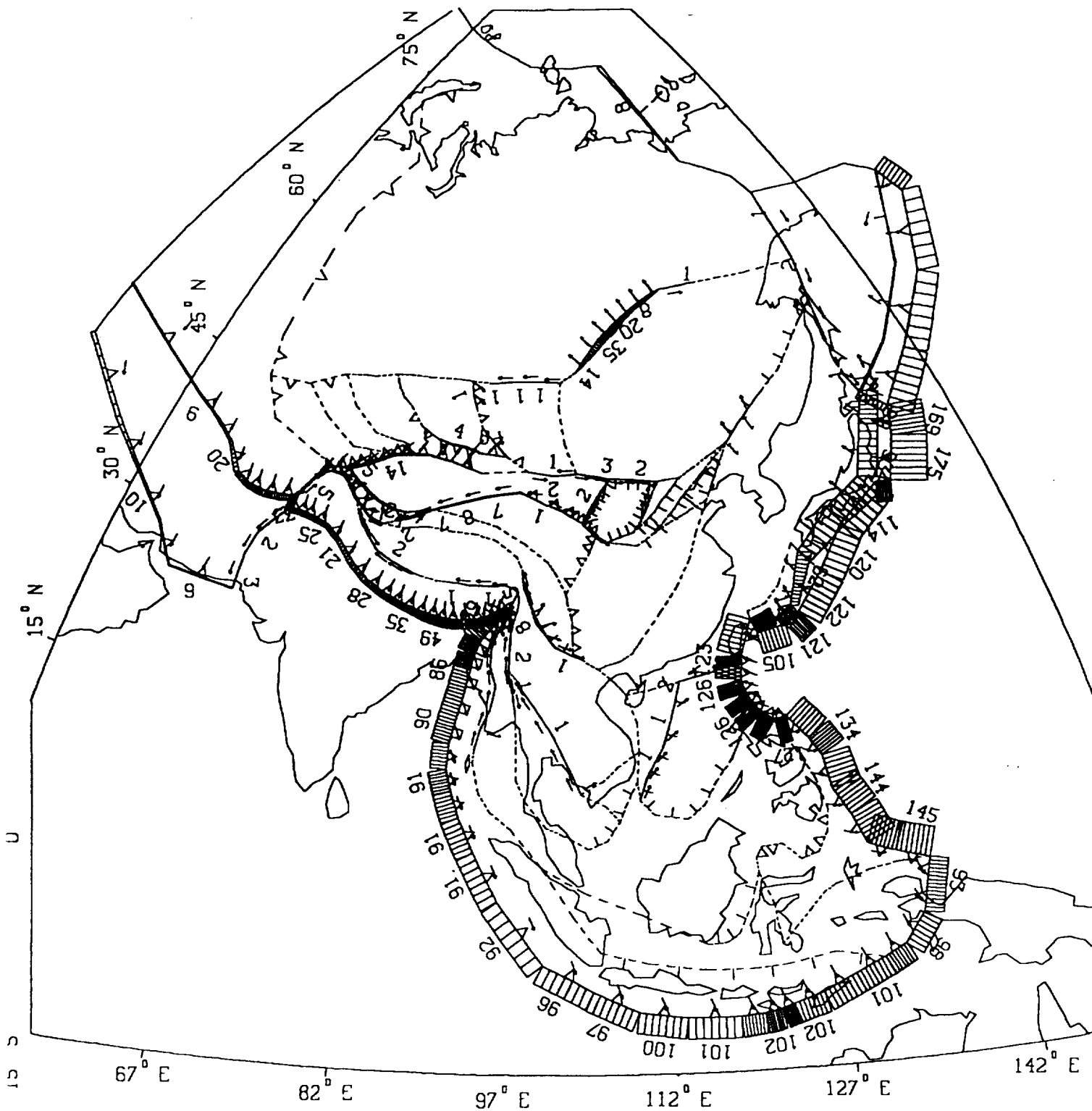
(5)

SURFACE VELOCITY
ASIAK9401: FAULTS 0.065, BLOCK 0.85, SBDCT 15 AND 2 MPA



→ 130.3 mm/year (6)

MEAN SLIP-RATE OF FAULTS
 ASIAK9401: FAULTS 0.065, BLOCK 0.85, SBDCT 15 AND 2 MPA



SLIP-RATE:

5



mm/year

LOCKED



DEXTRAL



SINISTRAL



THRUST

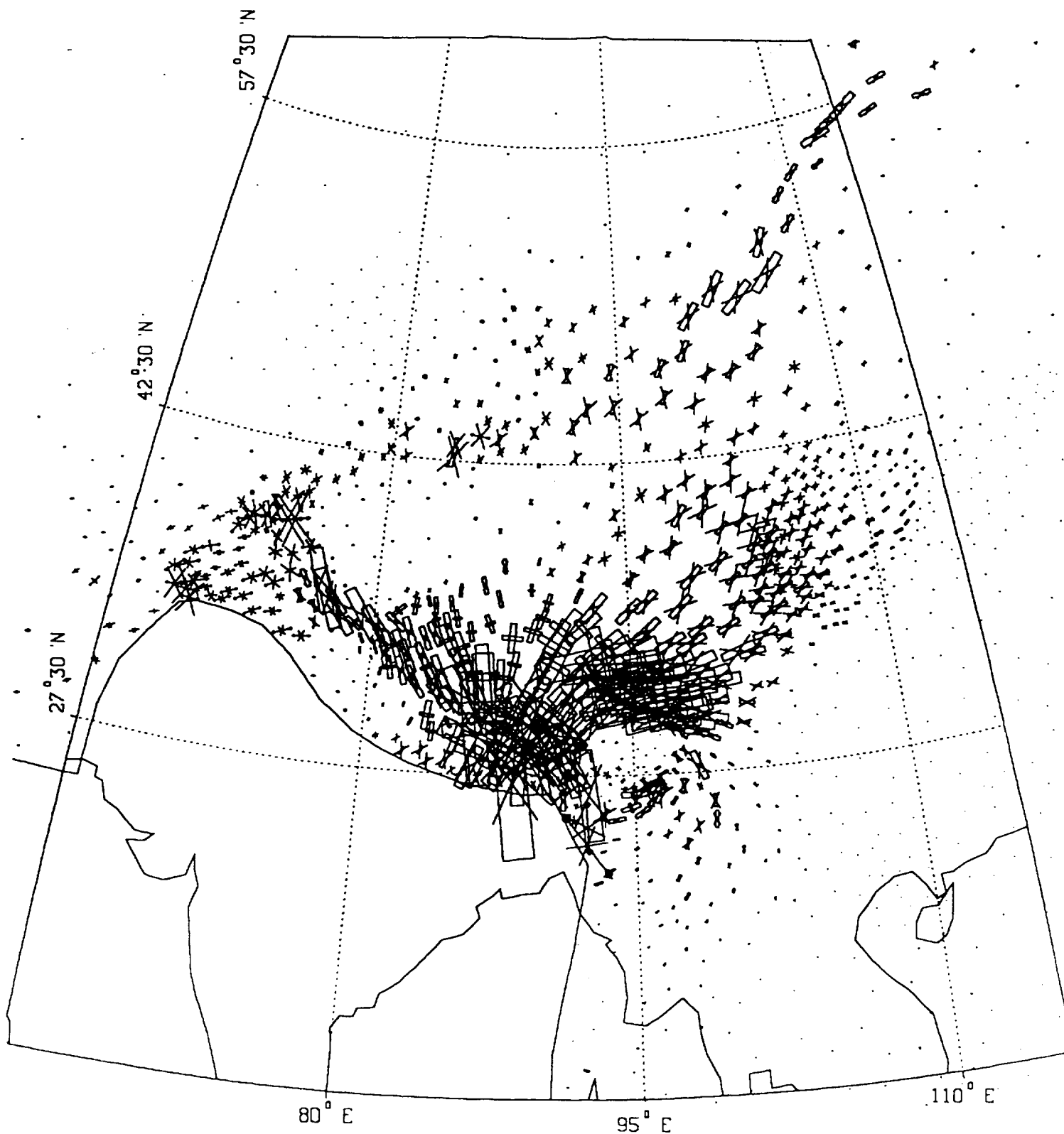


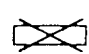
NORMAL



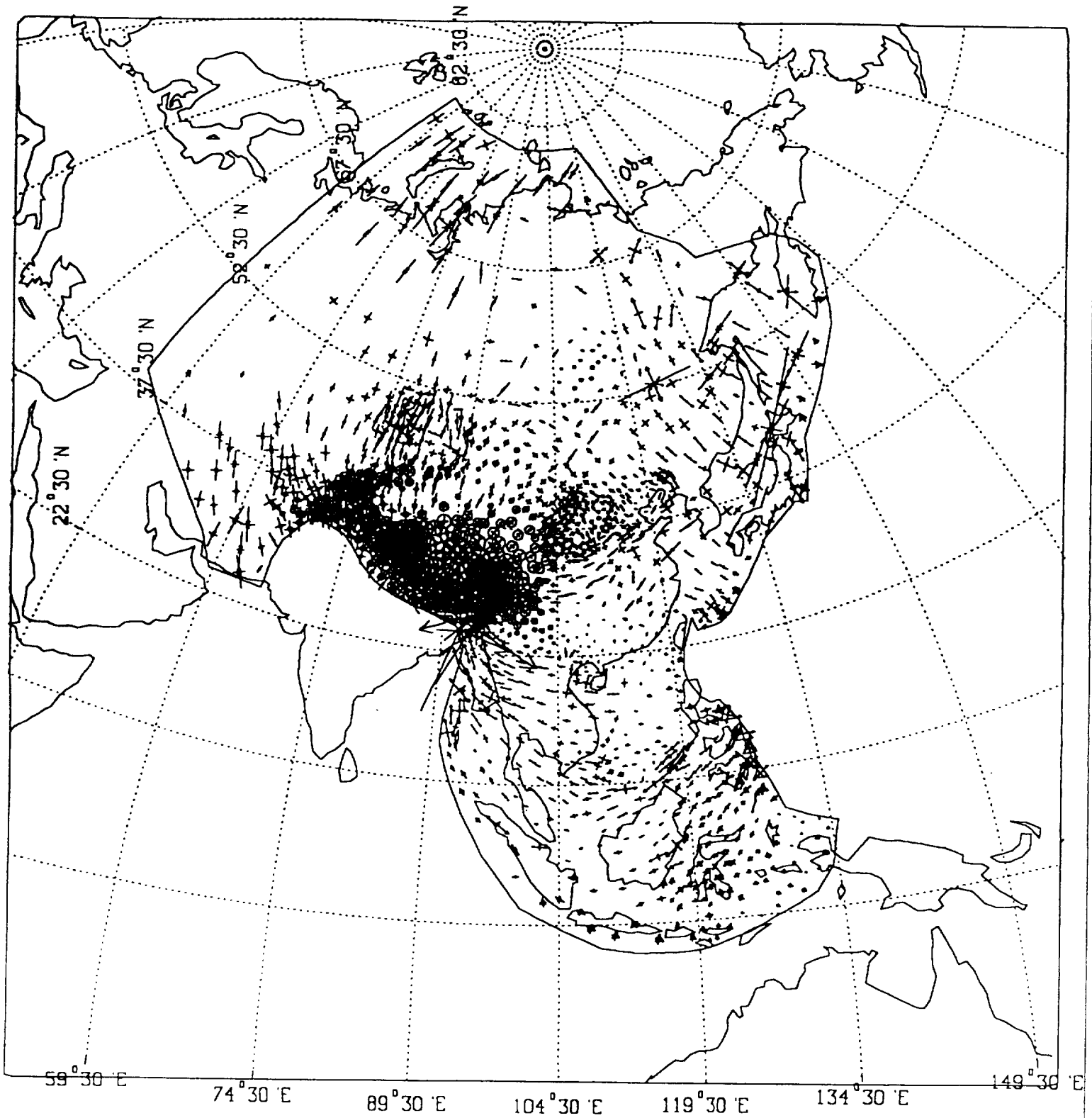
7


SURFACE STRAIN-RATE
ASIAK9401: FAULTS 0.065, BLOCK 0.85, SDOCT 15 AND 2 MPA



 $3.2 \times 10^{-15} /s$

VERTICALLY INTEGRATED DEVIATORIC STRESSES
ASIAK9401: FAULTS 0.065, BLOCK 0.85, SDOCT 15 AND 2 MPA



 2.0×10^{13} N/m

9